Effect of Heating Rate on Morphological Features of Oxidized Electroless Nickel–Boron Coatings

A. Chami[a],*, B. Nasiri-Tabrizi[b]

[a] *Department of Materials Engineering, Shahreza Branch, Islamic Azad University, Shahreza, Isfahan, Iran.*
[b] *Advanced Materials Research Center, Department of Materials Engineering, Najafabad Branch, Islamic Azad University, Najafabad, Isfahan, Iran.*

ARTICLE INFO

ABSTRACT

Due to their high hardness and wear resistance, electro less nickel-boron (Ni-B) coatings have found numerous applications. In the present study, the influence of the heating rate on the morphological features of oxidized electro less Ni-B coatings was investigated. The oxidation behavior of electro less coating layers was studied by TGA method under non-isothermal conditions at the heating rates of 5, 9 and 13°C/min. The phase compositions, elemental constituents, and microstructural characteristics were characterized by X-ray diffraction (XRD), energy dispersive X-ray spectroscopy (EDX), and scanning electron microscopy (SEM), respectively. Results showed that the morphological features of the oxidized coating were significantly influenced by the heating rate so that under the heating rate of 5 °C/min the morphology of the oxidized layer was a porous film with an average pore size of around 2 μm. With increasing the heating rate to 9 °C/min, more recessed pores or intervals were gradually overlaid by a film. Further increasing the heating rate to 13°C/min caused the formation of polygonal protuberances on the surface.

1. Introduction

In recent years, coatings and thin films are becoming more important across a wide range of industries [1]. With the advancement of science and engineering, the novel material concepts are successfully employed for various technologies such as coatings to optimize the functional properties-often with reduced material consumption, with low technical effort, and at low process costs [2]. In general, a metal can be deposited using aqueous solutions which can be broadly divided into two categories: electrolytic and electro less [3, 4]. In the electro less metal deposition process, no external current supply is required to deposit the material on a substrate. In fact, the electro less plating (EP) is an autocatalytic process where the substrate develops a potential as it is dipped in electro less solution called a bath that contains a source of metallic ions, reducing agent, stabilizer and other components [5].

Due to the developed potential, both positive and negative ions are attracted to the substrate surface and release their energy through charge transfer. It should be noted that each process parameter plays a specific role in the process and influences the process response variables [6].

Corresponding author:
E-mail address: Chami_akbar@yahoo.com (Akbar Chami).

During the last decade, the electro less deposition process has undergone numerous modifications to meet the challenging needs of a variety of industrial applications. Among the various types of electro less plating, electro less nickel (EN) has gained immense popularity due to its capability to provide a hard, wear and corrosion resistant surface [7]. The features of the EN process have made it a popular deposition process, with many widespread applications in the electronic packaging industry. The EN processes are grouped as Ni–P (EN–P), Ni–B (EN–B) and pure Ni, based on the reducing agents used (i.e., hypophosphite, borohydride or dialkyl aminoborane and hydrazine) in the plating bath [8]. EN–P plating has attracted particular attention for low-cost, flip chip bumping technology, which combines EN and immersion gold with solder printing techniques [9]. Other reasons for the popularity of EN–P in wafer bumping include the cost savings from mask less processing and batch processing, bump uniformity, superior diffusion barrier performance, slow growth rate of Ni–Sn intermetallic compounds (IMCs), and satisfactory solder ability [10,11]. Besides, borohydride- or dimethyl amineborane (DMAB)-reduced EN deposits have received considerable attention in recent years [8, 12]. The EN–B coating is more wear resistant than tool steel and hard chromium coatings [13], and possesses superior solder ability compared to the EN–P coating because its thin oxide layer can be penetrated by the solder [14]. According to literature, the characteristics of the EN–B deposits are known to be influenced by the processing parameters [2]. For example, Krishnaveni et al. [15] studied the relationship between the micro hardness of the electro less Ni-B coatings and heat treatment temperature and reported two maxima in the hardness versus heat-treatment temperature curve, one at 350 °C and the other at 450 °C. Beyond 450 °C, the coatings began to soften as a result of conglomeration of the Ni3B particles, and the hardness decreased. In another research, Dervos et al. [16] achieved a chromium equivalent hardness (more than 1600 HV) by heat treating the Ni-B films in high vacuum. The high hardness of electro less Ni-B plating

has been utilized in the fabrication of micro-metal molds [17]. There are some investigations about the corrosion resistance of the Ni-B electro less coatings [18-20] but there is few published work about the oxidation behavior of Ni-B electro less coating at high temperatures. Tomlinson and Wilson [21] studied the oxidation of electro less Ni-B and Ni-P coatings in air at 800 to 1000°C and showed that all kinetics followed the parabolic oxidation law and the rate increased in the order spectrographically pure nickel, commercially pure nickel, Ni-B, and Ni-P, with the Ni-P oxidizing approximately 1000 times faster than the spectrographically pure nickel. To the best of our knowledge, scientific approaches to investigate the influence of the heating rate on the morphological features of the oxidized Ni-B films have remained unaddressed. Therefore, in the present study, the effect of the heating rate on the microstructural evolutions of oxidized electro less Ni-B coatings was explored.

2. Materials and methods

In the present study, medium carbon steel (AISI 1045 grade, 60 mm×30 mm×1 mm) was utilized as substrate for the deposition of electro less Ni-B coatings. The substrate was degreased using acetone. Since carbon steel substrate is not catalytically active, deposition of electro less Ni–B coatings will not occur unless these substrates are activated. A nickel strike using Watt's or Wood's nickel bath is usually employed to activate the non-catalytic metallic substrates prior to their immersion in the electro less plating bath [8]. In this research, a Watt's nickel bath has been used to activate the stainless steel substrate. To prepare the electro less Ni–B deposits, an alkaline bath containing nickel chloride ($NiCl_2$) as the source of nickel and sodium borohydride ($NaBH_4$) as the reducing agent was used. In addition to these materials, the plating bath was composed of suitable quantities of ethylenediamine ($C2H_4(NH_2)_2$) and disodium tartrate ($C_4H_4Na_2O_{6.2}(H_2O)$) as complex agents and thallium acetate as the stabilizer. During the plating, the temperature of the bath was maintained at 45±1 °C. In addition, the bath solution was agitated

Table 1. Concentrations and operating conditions of electro less Ni-B plating

Bath composition	
Nickel chloride	30 g/l
Ethylenediamine (98%)	15 g/l
Disodium tartrate	40 g/l
Sodium hydroxide	40 g/l
Sodium borohydride	0.2 g/l
Thallium acetate	16 mg/l
Operating conditions pH	13
Temperature	45±1 °C

using a magnetic stirrer at 600 rpm. The concentrations and operating conditions of the electro less Ni-B plating are summarized in Table 1.

The oxidation behavior of the deposited layer was investigated by non-isothermal thermo gravimetric method. A Mettler Tuledu Star System was used for simultaneous TGA studies. The experiments were performed under non-isothermal condition at programmed linear heating rates of 5, 9 and 13 °C/min. The range of temperature was 25–1200 °C. Oxygen flowing was used for oxidation and the flow rate was maintained at 30 ml min−1.

X-ray diffraction (Philips X–ray diffractometer (XRD), Cu–Kα radiation, 40 kV, 30 mA and 0.02 °S−1 step scan) was employed to evaluate the phase purity and the crystallographic structural properties of the coatings before and after the oxidation. The XRD patterns were collected over the 2θ angular range between 30° and 80° at the scan speed of 1°/min. "PANalyticalX'PertHighScore" software was used to analyze the XRD data. The XRD patterns were compared to the standards compiled by the Joint Committee on Powder Diffraction and Standards (JCPDS), which involved card #004-0850 for Ni and #048-1223 for Ni_3B. Morphological features of the specimens were examined by scanning electron microscopy (SEM; MIRA©TESCAN, Czech Republic) at the acceleration voltage of 15 kV. X-ray energy dispersion spectroscopy (EDS) attached to the SEM was utilized for semi-quantitative examination of the samples.

3. Results and discussion

Fig. 1 shows the XRD profiles of electro less Ni–B coating before and after oxidation with different heating rates (5, 9 and 13 °C/min). As can be seen, after electro less plating, the substrate was fully covered by the Ni-B alloy. However, the diffraction pattern of the Ni–B alloy had a single broad peak at 2θ = 44.65° and the reflections corresponding to the (1 1 1) plane of a face-centered cubic (fcc) phase of nickel could be observed. This showed that the structure of the as-deposited Ni-B coating was amorphous nickel, which was composed of boron analyzed by EDS. According to the literature, in the electro less deposition process, the extent of segregation of metalloid alloy in the coating affects its crystallinity (fraction of crystalline phases) [18]. Therefore, the appearance of this amorphous structure of the Ni-B layer can prove that nucleation of the nickel phase was inhibited and required that boron segregation was large enough. Upon non-isothermal oxidation with different heating rates, the Ni–B coating was crystallized and as a result the existence of boron in the as−plated Ni-B layer was intensified. This is expected from the previous results [3].

After oxidation with the heating rate of 5 °C/min, the existence of Ni together with minor Ni_3B was verified. In fact, the phase composition included Ni and Ni3B.With the increase of the heating rate to 9 and 13 °C/min, similar phase constituents were observed and no phase transition was detected. However, some boron oxide may be formed during the
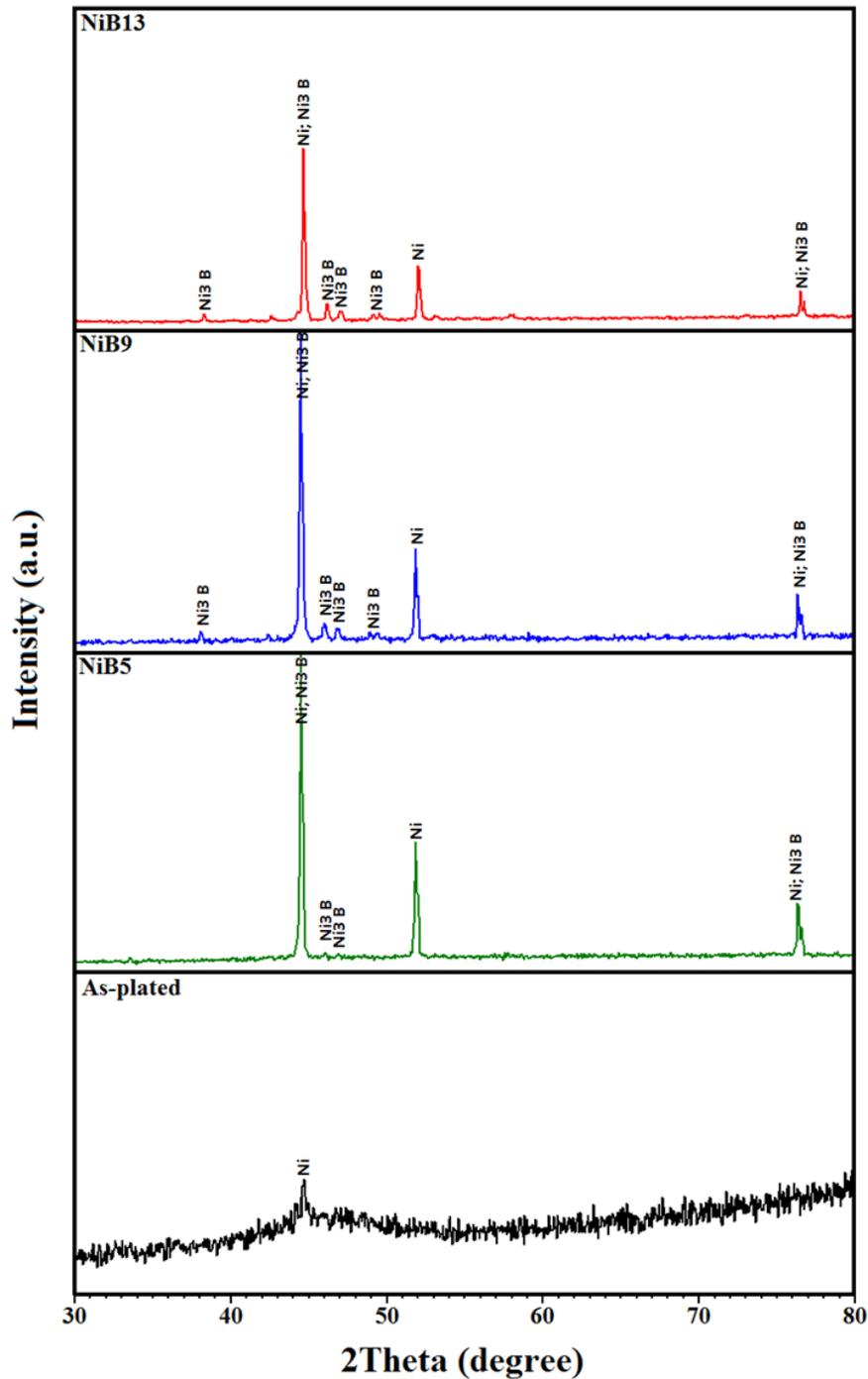
Fig. 1. XRD profiles of the electroless Ni–B coating before and after non-isothermal oxidation at different heating rates (5, 9 and 13 °C/min)

process which may be evaporated due to the high vapor pressure at high temperatures. From the structural point of view, with increasing the rate of heating, some distinct features can be identified. First, the intensity of the characteristic peaks of Ni and Ni3B

significantly decreased which is believed to be caused by the amorphization of the coating. Second, some set of reflections for both Ni and Ni_3B phases gradually shifted toward higher angles. This behavior probably resulted from the relaxation of residual compressive stress
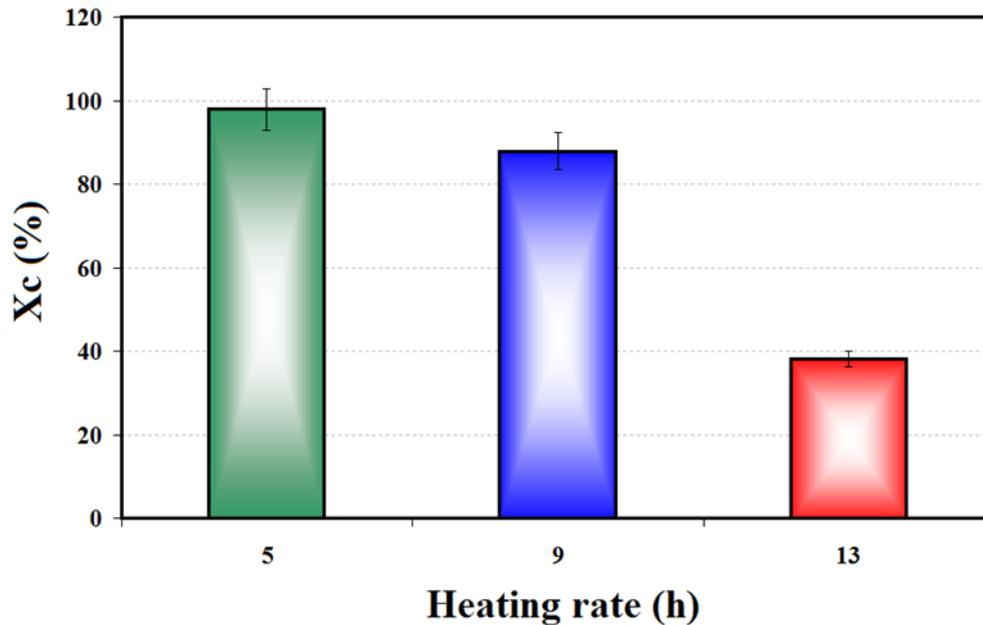
Fig. 2. The crystallinity degree of the electro less Ni–B coating before and after non-isothermal oxidation at different heating rates (5, 9 and 13 °C/min)

during the process which is in good agreement with the previous studies [22].

The degree of crystallinity (Xc) of the coatings as fraction of crystalline phase was estimated by taking the sum total of relative intensities of the characteristic peaks of Ni for the samples ((I1: In) Ni) and standard ((I1: In) Standard) using the following equation [23]:

$$X_C = \frac{\text{Sum}\left(I_1 : I_n\right)_{Ni}}{\text{Sum}\left(I_1 : I_n\right)_{Standard}} \times 100 \qquad [1]$$

The crystallinity degree (Xc) of the electro less Ni–B coatings at different heating rates 5, 9 and 13°C/min are shown in Fig. 2. As can be seen, the crystallinity degree of the coating was around 97% with the heating rate of 5 °C/min. With increasing the heating rate to 9 °C/min, the crystallinity degree decreased to 87% and reached a minimum about 38 % when the heating rate increased to 13 °C/min. From the XRD profiles, an increased broadening of the Ni (1 1 1) reflection was observed, suggesting that the crystallinity degree has changed by changing the heating rate of plating. Similar results have also been observed in the literature [24, 25]. Gaevskaya et al. [24] reported a decrease in the intensity of the Ni (1 1 1) reflection and an increase in its half-width with increasing the B content in the EN–B plating layer. Kumar and Nair [25] observed an increased sharpness of the XRD profile with decreasing the B content in the EN–B plating layer due to the increased coating crystallinity. Here, the decrease in the crystallinity degree was most probably due to the reduction in the duration of the samples exposure to high temperature whereas the heating rate increased from 5 to 13 °C/min.

The surface morphology of the as-plated electro less Ni–B deposit is shown in Fig. 3, which demonstrates a smooth surface morphology with good uniformity and typical cube-shaped particles. After non-isothermal oxidation, the morphological features of the coating were noticeably changed by increasing the heating rate as shown in Fig. 4. In general, the oxidation process is expected to result in a dense layer, but in this case the formation of a porous structure was dominant which could be due to the removal of gas (boron oxide) from the system. As can be seen in Fig. 4a, the porous film had an average pore size of around 2 μm during the heating rate of 5 °C/min. Besides, the microstructure exhibited a bimodal grain size distribution characterized by the
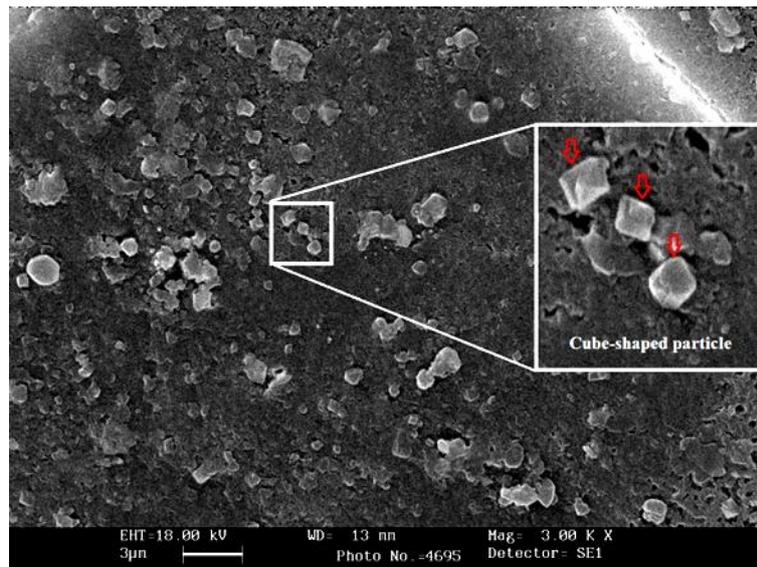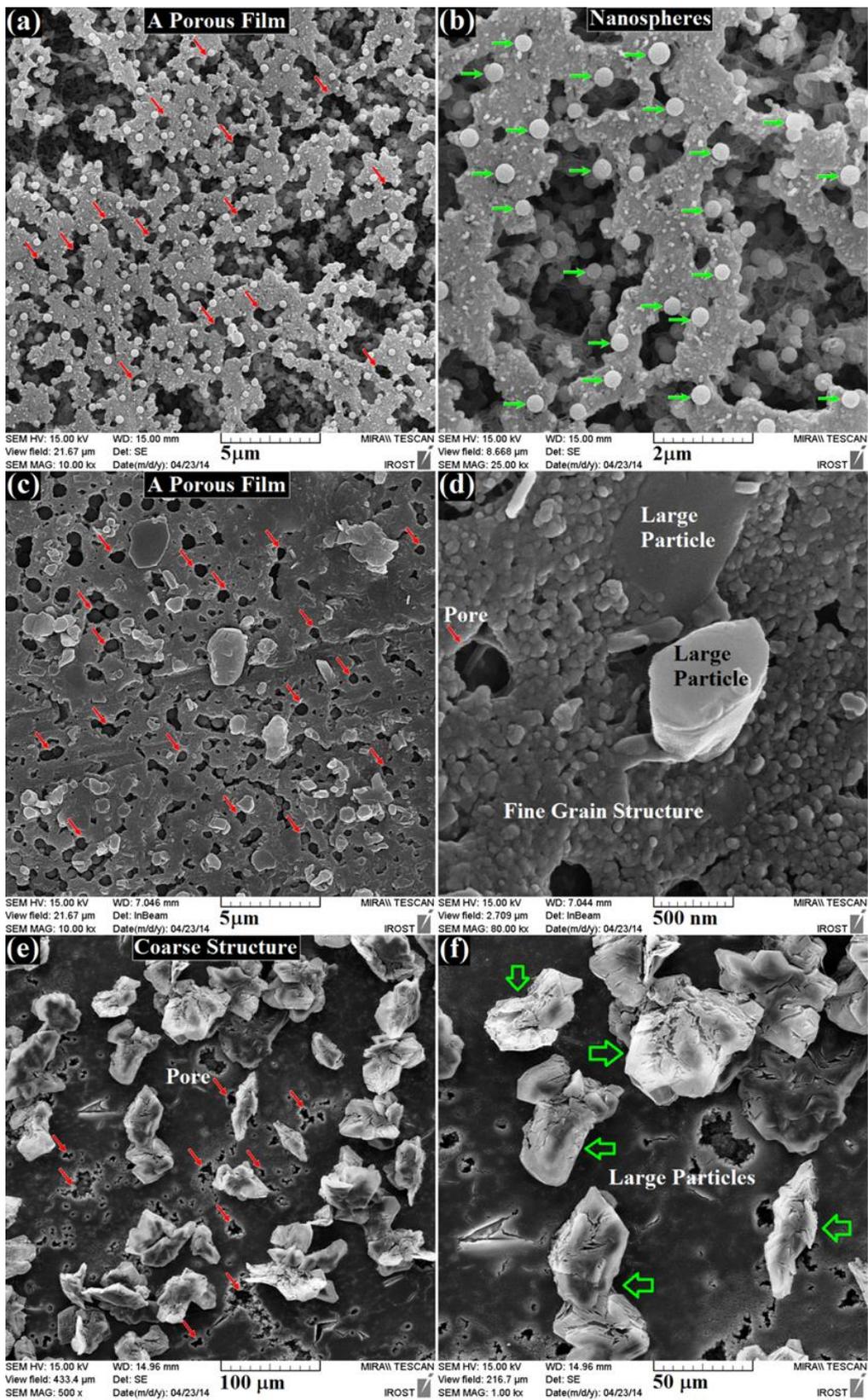
Fig. 3. SEM image of the electro less Ni–B coating before non-isothermal oxidation

presence of Nano spheres with the average size of about 300±15 nm along with finer grains with the mean size of around 80±4 nm (Fig. 4b).

With increasing the heating rate to 9 °C/min (Fig. 4c and d), significant changes in the microstructural features were observed so that the volume fraction and size of pores (0.7 μm) declined obviously. Moreover, the initial spherical particles were gradually converted to coarse angular particles with the mean size of about 1 μm. Further increasing the heating rate to 13 °C/min resulted in the formation of polygonal protuberances on the surface of the sample (Fig. 4e). In this case, large-size particles agglomerated to form coarse clusters as shown in Fig. 4f.

In addition, in some uncovered pores, crowded distribution of fine particles is still visible. These differences in morphological characteristics were quite likely due to the changes in the atomic diffusion. As a matter of fact, in the solid state crystal, diffusion within the crystal lattice takes place by either interstitial or substitutional mechanisms and is referred to as lattice diffusion [26]. In interstitial lattice diffusion, a penetrating agent will diffuse in the lattice structure of a crystalline structure, while in substitutional lattice diffusion (self-diffusion for example), the atom can only move by substituting place with another atom. Substitutional lattice diffusion is often contingent upon the availability of point vacancies throughout the crystal lattice. Owing to the prevalence of point vacancies raises in accordance with the Arrhenius equation, the rate of crystal solid state diffusion increases with temperature. Hence, with increasing the heating rate from 5 to 13 °C/min, a reduction in the duration of exposure to high temperature was required for the occurrence of atomic diffusion which led to change in the morphology of particles from spherical structure to polygonal structure.

Fig. 4. SEM images of the electro less Ni–B coating after non-isothermal oxidation at different heating rates; (a and b) 5, (c and d) 9 and (e and f) 13 °C/min

In the present study, the EDS analysis was executed for several samples from which typical profiles have been selected and presented in Fig. 5. To provide more precise data, the EDS analysis was recorded over three different points on the samples. In accordance with the EDS profile in Fig. 5, boron, nickel and oxygen are the main elemental constituents of the coatings. Due to the strong absorption of the boron Kα line, this element was observed with high relative error. Furthermore, the appearance of the Au peaks with high density in the selected areas was due to the gold films for the SEM analysis. According to the EDS spectra, no chemically stable impurity was formed during the non-isothermal oxidation. From the EDS analysis and the inset tables in this figure, it is obvious that the weight/atomic percentage of oxygen are dominant in all spectra which can be attributed to the formation of boric acid. In the case of oxidation with the heating rate of 5 °C/min, there was enough time for atomic diffusion and accordingly the evaporation caused a constant particle size. In contrast, with increasing the heating rate up to 13 °C/min, due to the insufficient time for the atomic diffusion, a coarse structure was formed.
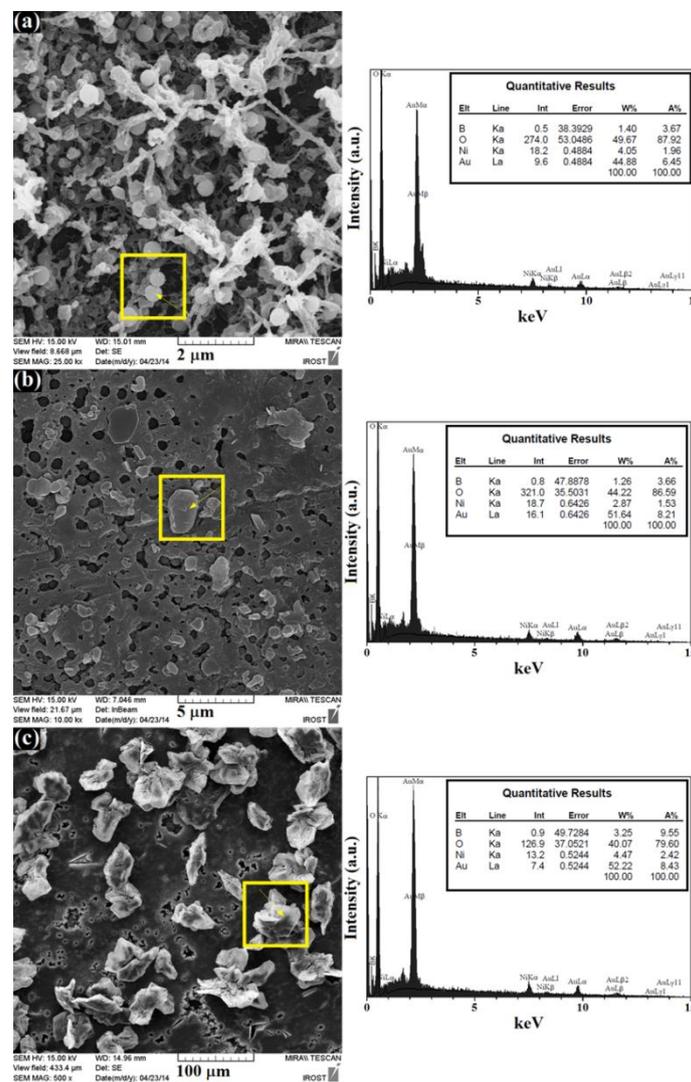
Fig. 5. The EDX spectra of electro less Ni–B coating after non-isothermal oxidation at different heating rates; (a) 5, (b) 9 and (c) 13 °C/min

4. Conclusion

In the present study, the effect of the heating rate on the morphological features of the oxidized electro less nickel-boron plating was explored. With increasing the rate of heating, some distinct features can be identified in the XRD profiles. From the SEM observations, a porous structure with an average pore size of around 2 μm was formed during oxidation with the heating rate of 5 °C/min. In this case, the microstructure showed a bimodal grain size distribution characterized by the presence of Nano spheres with the average size of about 300 ± 15 nm along with finer grains with the mean size of around 80 ± 4 nm. With increasing the heating rate to 9 °C/min, significant changes in the microstructural features were observed so that the volume fraction and size of pores (0.7 μm) declined obviously. Further increasing the heating rate to 13 °C/min caused the formation of polygonal protuberances on the surface of the sample. Based on the EDS spectra, no chemically stable impurity was formed during the non-isothermal oxidation. The obtained results showed that in the case of oxidation with the heating rate of 5 °C/min, there was enough time for atomic diffusion and accordingly the evaporation caused to a constant particle size. On the contrary, with the increase of the heating rate up to 13 °C/min, due to the insufficient time for the atomic diffusion, a coarse structure was detected.

Acknowledgment

References

1. R. C. Agarwala, V. Agarwala, Electroless alloy/composite coatings: a review, Sadhana, Vol. 28, 2003, pp. 475–493.
2. S. Kalyan Das, P. Sahoo, Influence of process parameters on microhardness of electroless Ni-B coatings, Advances in Mechanical Engineering 2012, 2012, pp. 1-11.
3. W. Riedel, Electroless nickel plating. Stevenage, Hertfordshire, UK: Finishing Publications Ltd, 1991.
4. M.V. Ivanov, Electroless nickel–boron–phosphorus coatings: protective and functional properties, Prot Met (Translated from ZashchitaMetallov), Vol. 37, 2001, pp. 592–6.
5. F. Delaunois, J. P. Pelitjean, P. Lienard and M. Jacob-Duliere, Autocatalytic electroless nickel–boron plating on light alloys, Surface and Coatings Technology, Vol. 124, 2000, pp. 201–9.
6. B. Oraon, G. Majumdar and B. Ghosh, Improving hardness of electroless Ni–B coatings using optimized deposition conditions and annealing, Materials & Design, Vol. 29 2008, pp. 1412-1418.
7. K. Krishnaveni, T. S. N. Sankara Narayanan and S. K. Seshadri, Electroless Ni–B coatings: preparation and evaluation of hardness and wear resistance, Surface and Coatings Technology, Vol. 190, 2005, pp. 115-21.
8. Baskaran, R .S. Kumar, T. S. N. Sankara Narayanan and A. Stephen, Formation of electroless Ni–B coatings using low temperature bath and evaluation of their characteristic properties, Surface and Coatings Technology, Vol. 200, 2006, pp. 6888–94.
9. J. H. Lau, Low Cost Flip Chip Technologies for DCA, WLCSP, and PBGA Assemblies, McGraw-Hill, New York, 2000.
10. J. Simon, E. Zakel and H. Reich, Proceedings of the 40th Electronic Components and Technology Conference, New York, 1990, pp. 412–417.
11. J. W. Yoon, S. B. Jung, Effect of isothermal aging on the interfacial reactions between Sn–0.4Cu solder and Cu substrate with or without ENIG plating layer, Surface and Coatings Technology, Vol. 200, 2006, pp. 4440–4447.
12. J. Woong Choi, G. Ho Hwang, W. Kyu Han and S. Goon Kang, Phase transformation of Ni–B, Ni–P diffusion barrier deposited electrolessly on Cu interconnect, Applied Surface Science, Vol. 253, 2006, pp. 2171–8.
13. R. N. Duncan, T. L. Arney, Performance of electroless nickel coatings in food products, Plating and Surface Finishing, Vol. 71, 1984, pp. 49–54.
14. Y. M. Chow, W. M. Lau and Z. S. Karim, Surface properties and solderabilitybehaviour of nickel-phosphorus and nickel-boron deposited by electroless plating, Surface and Interface analysis, Vol. 31, 2001, pp. 321–7.
15. K. Krishnaveni, T. S. N. Sankara Narayanan and S. K. Seshadri, Electroless Ni-B coatings: preparation and evaluationof hardness and wear resistance, Surface and Coatings Technology, Vol. 190, 2005, pp. 115–121.
16. C. T. Dervos, J. Novakovic and P. Vassiliou, Vacuum heat treatment of electroless Ni-B

coatings, Materials Letters, Vol. 58, 2004, pp. 619–23.

17. Y. Sawa, K. Yamashita, T. Kitadani, D. Noda and T. Hattori, Fabrication of high hardness Ni mold with electro less nickel boron thin layer, Microsystem Technologies, Vol. 16 2010, pp. 1369–75.

18. W. X. Zhang, Z. H. Jiang, G. Y. Li, Q. Jiang and J. S. Lian, Electro less Ni-P/Ni-B duplex coatings for improving the hardness and the corrosion resistance of AZ91D magnesium alloy, Applied Surface Science, Vol. 254 ,2008, pp. 4949-4955.

19. T. S. N. Sankara Narayanan, K. Krishnaveni and S. K. Seshadri, Electro less Ni-P/Ni–B duplex coatings: preparation and evaluation of micro hardness, wear and corrosion resistance, Materials Chemistry and Physics, Vol. 82, 2003, pp. 771-779.

20. L. Wang, L. Zhao, G. Huang, X. Yuan, B. Zhang and J. Zhang, Composition, structure and corrosion characteristics of Ni–Fe–P and Ni–Fe–P–B alloy deposits prepared by electro less plating, Surface and Coatings Technology, Vol. 126, 2000, pp. 272-278.

21. W. J. Tomlinson and G. R. Wilson, The oxidation of electro less Ni-B and Ni-P coatings in air at 800 to 1000 °C, Journal of Materials Science, Vol. 21, 1986, pp. 97-102.

22. S. Komiyama, Y. Sutou and J. Koike, Effect of heat treatment on the hardness of Ti-Mo-N films deposited by RF reactive magnetron sputtering, Materials Transactions, Vol. 51, 2010, pp. 1467–73.

23. S. S. Rayalu, J. S. Udhoji, S. U. Meshram, R. R. Naidu and S. Devotta, Estimation of crystallinity in flyash-based zeolite-A using XRD and IR spectroscopy, Current Science, Vol. 89, 2005, pp. 2147–51.

24. T. V. Gaevskaya, I. G. Novotortseva and L. S. Tsybulskaya, The effect of boron on the microstructure and properties of electrodeposited nickel films, Metal Finishing, Vol. 94, 1996, pp. 100–3.

25. P. S. Kumar and P. K. Nair, X-ray diffraction studies on the relative proportion and decomposition of amorphous phase in electroless Ni-B deposits, Nanostructured Materials, Vol. 4, 1994, pp. 183–98.

26. P. Heitjans, J. Karger, Diffusion in condensed matter: methods, materials, models (2nd ed.). Birkhauser, eds. 2005.